

ASSESSMENT TECHNIQUES FOR ALKALI-SILICA REACTION DIAGNOSIS IN MASS CONCRETE STRUCTURE

* Suvimol Sujjavanich¹, Thanawat Meesak¹, Krit Won-in² and Viggo³

¹Faculty of Engineering, Kasetsart University, Thailand; ²Faculty of Science, Kasetsart University, Thailand; ³Norwegian Concrete and Aggregate Laboratory Ltd., Trondheim, Norway

*Corresponding Author, Received: 17 Oct. 2018, Revised: 28 Dec. 2018, Accepted: 12 Jan. 2019

ABSTRACT: This paper reported the results of several techniques used to diagnose Alkali-Silica Reaction (ASR) distress in concrete. Two screening tests looked for the appearance of the fluoresced gel of uranyl acetate treated samples and the changed color areas of the chemical staining treated samples. The results agreed well with the expansion of the cored samples in warm water and in NaOH solution and also supported the previously measured expansion in the field. The petrographic analysis found many microcracks with ASR gel filling in cement paste, interface zone (ITZ) between aggregates and paste, and internal cracks in aggregates. Microstructural analysis revealed the characteristics of slow reactive aggregates and two forms of products; amorphous gel with shrinkage cracks in cement paste cracks and in the ITZ, and cryptocrystalline reaction products consisting of plate-formed crystals, rosettes and globular found mostly in internal cracks of aggregates and air voids. The SEM/EDS analysis differentiate reactive from non-reactive aggregates. Ettringite crystals were also observed lining the air voids and some cracks but there was no evidence linking it to the cause of continued expansion. Fine grain black quartzite within the aggregates and sericite were identified as the cause of ASR. The combination of different techniques effectively identified ASR as the primary cause of deterioration and the continued expansion of the investigated structure.

Keywords: ASR, Screening, Petrographic, Accelerated, Microstructural Analysis

1. INTRODUCTION

Alkali-silica reaction (ASR) has been globally recognized since 1940. Since then numerous researches have been conducted on the mechanisms, assessment, and mitigation [1-3]. Because the problem is naturally complicated and some symptoms look alike to those of other problems, to identify the cause and severity is important but difficult and need expertise, time and expenses [4].

Several qualitative and quantitative methods have been proposed for ASR assessment. Some are widely accepted as standard methods. However, because of the strength and weakness of each individual method, none is accepted as one sole method that is capable of definitive identification of the problem [5,6].

The first ASR-related problem in Thailand in the mass foundation of a large infrastructure project was reported in 2009 [7, 8]. During the first 10 years of service visual inspections reported extensive cracks of about 20% of the surveyed footings and the continued expansion in the mass foundations. The typical grid pattern cracks of about 0.50 m apart, accompanied by randomly finer cracks [7]. Several causes of distress were eliminated and finally, the two most suspicious causes, namely ASR and DEF or Delayed Ettringite Formation, were focused on and that led to a detailed investigation to confirm the root cause of the problem.

The expansion and cracking are characteristics of both ASR and DEF but the causes are different. ASR originates from unstable forms of silica in aggregates reacting with alkalis, in particular, hydroxyl ions in pore solution, which is directly related to the amount of sodium and potassium in cement. The product of this reaction, the alkali-silica gel, is capable of imbibing water from the surrounding, then expands and causes cracking or other defects as reported worldwide [9]. On the other hand, DEF is an internal sulfate attack caused by ettringite formation in hardened concrete.

Moreover, several factors were found to be related to DEF occurrences such as sulfate in clinker, high temperature, alkali and water [10,11]. Both ASR and DEF can cause expansion, cracks and are often found in the same structure. The causes, timeline of occurrence and the possible correlation of these two processes are still being researched.

Due to these complications, six techniques were employed to identify the main cause of deterioration of this case. These included: two screening tests, expansion test, microstructural and petrographic analysis, and SEM/EDS. This paper presents the experimental details and the results to provide an accurate diagnosis of the premature deterioration.

2. STUDY PROGRAM

Thirty-three concrete samples of 75 mm in diameter and 500 mm in length were randomly cored from 12 footings, in the vertical and the horizontal direction. After coring, all samples were carefully wrapped with paper and plastic wrap and then kept in air-tight plastic bags for later investigation processes. After a visual inspection in the laboratory, samples were cut into 75mm in diameter and 150mm in length for compression tests, to determine the concrete strength after ten years of service. Some were used for the screening tests and other investigations to investigate the main cause as explained below.

2.1 Screening Test

Two simple qualitative methods namely, uranyl acetate solution and a geochemical staining method were applied on the freshly-cut surfaces of concrete discs to detect the evidence of alkali-silica gel. The first aimed to observe, under ultraviolet light, fluoresced greenish-yellow rim of the uranyl ions absorbed by negative ions in the gel [12]. However, the fluorescence may also be found from ettringite as well as in concrete affected by carbonation. The second, solutions of sodium cobaltinitrite and rhodamine-based were used to stain and detect K-rich Na-K-Ca-Si gels and alkali poor Ca-Si gels [13].

2.2 Accelerated Expansion Test

The cored samples of 150 mm in length, from different locations, were submerged in water at 38°C for 24 hours then reference lengths were measured. The specimens were then put in two accelerating conditions, the first was warm water at 38°C, and the second was 1M NaOH at 80°C. Expansions were measured at regular interval up to until 64 days.

2.3 Microstructural Analysis, Petrographic Analysis And SEM/EDS

For the first part, the thin slabs of about 10 mm thickness were cut parallel to the longitudinal axis of the core samples, impregnated with fluorescence dye and investigated visually and by stereomicroscope under both ordinary polarizing and fluorescence light. To prepare specimens for the second part, the concrete samples were cut at the depth about 0.5-1cm below the surface, to avoid the carbonated part of the concrete. Polished thin sections (TS) were carefully prepared to the thickness of 20 microns and carefully examined under a polarizing microscope mounted with UV filters. The prepared polished thin sections were

then coated with carbon and also examined with SEM/EDS technique, using Scanning Electron Microscope LEO 1450 VP mounted with an Oxford Instrument model 7366 EDS.

3. RESULTS AND DISCUSSIONS

3.1 Screening Test

From uranyl acetate test, the 8 out of 10 concrete samples showed the greenish-yellow rims under UV light around some coarse aggregates, in some internal cracks and often extended to cement paste as shown in Fig.1a. The different amount of the observed gels and their observed characteristics indicated different severity levels. The accumulated fluoresced glow found in some specific areas, as in Fig.1b, may indicate the potential collection of gel in the vicinity of the aggregates and the severe local reactivity. The evidence from this test was confirmed with the geochemical test in Fig.1c.

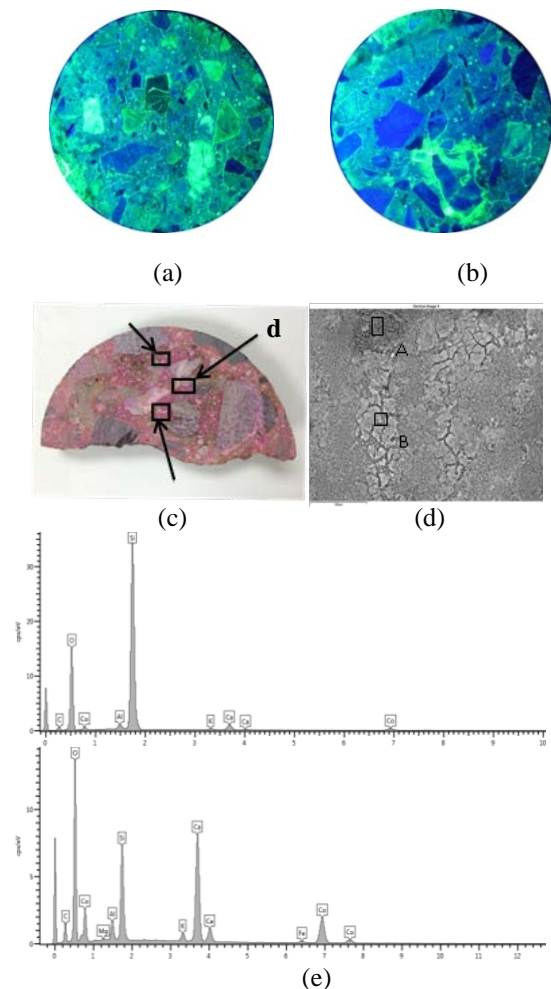


Fig.1 samples under UV light in uranyl acetate test, (a) high severity (b) very high severity, (c) different stain colors from the geochemical test, (d) specified area for SEM/EDX, (e) EDX analysis of areas A and B in (d)

The area “d” in the geochemical staining test in Fig.1c was investigated by SEM as shown in Fig.1d. EDX analysis was performed on areas “A” and “B”, showing a high amount of Ca, Si, and O in the pink area from the staining test, particular high Si in "A" and high Ca in "B"

3.2 Accelerated Expansion Test

The expansion under both accelerated conditions agreed well with the screening test results, particularly from the uranyl acetate test. The calculated reactive aggregates area of the companion samples from the same core in Table 1, agreed well with the expansion in Fig.2 [14].

Table 1 Percentage of calculated area of reactive aggregates

C- ID	React.agg.		Non react.agg.	
	Area, (cm ²)	%	Area, (cm ²)	%
A	6.9	47.3	7.7	52.7
C	1.0	8.1	11.3	91.9
D	10.5	65.9	5.4	34.1

Note: C- ID= core ID

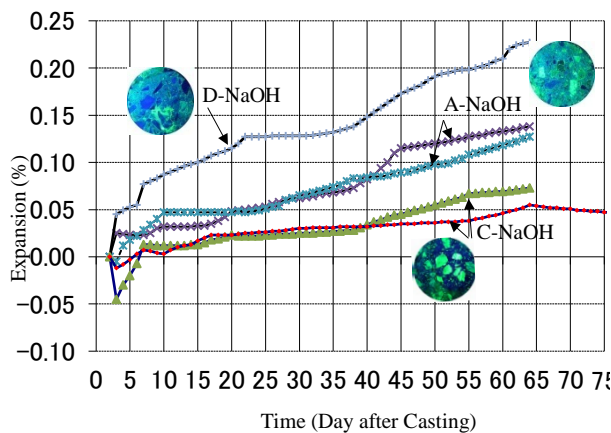


Fig.2 Expansion of core samples in different accelerated conditions [7]

Because both high temperature and alkali environment accelerated ASR reactivity of aggregates but not DEF, therefore a large expansion of samples A and D in 1M NaOH at 80°C confirmed the occurrence of ASR and not DEF. The results supported the continued expansion observed in the field. Warm water promoted both ASR and DEF, but the alkali leaching effect may retard ASR while accelerating DEF [14]. The much smaller expansion of sample C in similar conditions and even the observed shrinkage in warm water confirmed the small effect of ASR.

3.2 Microstructural Analysis

Analysis of the thin slab showed cracks in the cement paste, Interfacial Transition Zone (ITZ) around reactive aggregates and inside the aggregates. Several microcracks in reacted coarse aggregates sometimes continued into the cement paste and connected between aggregates as shown circled in Fig.3a, suggesting an advanced stage of detrimental ASR. The high intensity of microcracks in paste was also observed. This confirmed the findings from the screening tests in most ASR-affected samples. Two special features, similar to those of widely reported in slow reactive aggregates [15], were also observed in TS sample under the fluorescence light shown in Fig.3b. Lots fine cracks were observed near the edge of aggregate and the existence of the outer dense zone, shown by the arrow. Under polarized light shown in Fig.3c, the crack inside reacted aggregate connected to the paste and brownish reaction products (arrows) was observed. Cryptocrystalline reaction products were observed in some reacted aggregates but an insignificant amount of amorphous gel was found except in the contact zone near the cement paste. Ettringite in cracks in cement paste (arrows) was also observed.

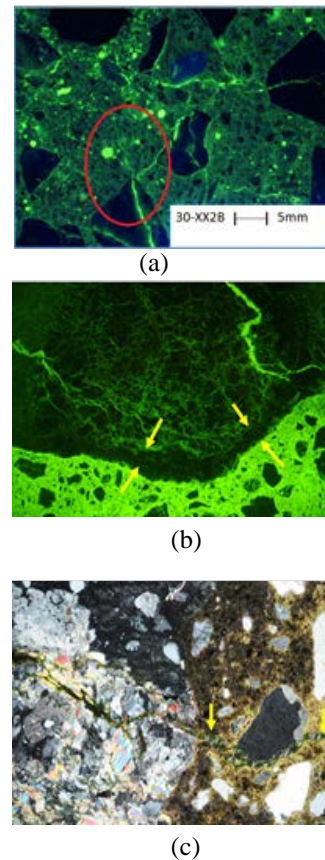


Fig.3 (a) cracks in the paste, around ITZ and inside aggregates (b) the dense zone in reactive aggregate and internal microcracks (c) continued aggregate's crack into a paste

3.3 Petrographic Analysis

The investigated polished thin sections (TS) showed that the majority of the coarse aggregates were granitic rocks, quartz with mica traces and sericite contained feldspar, quartz, and muscovite. Black quartzite with pyrite was also observed in samples. Typical microcracks of a 10-25 micron wide in the cement paste and filled with ASR gel were observed as well as cracks in ITZ as shown by arrows in Fig.4a. Delayed ettringite formation (DEF) was also found in both air voids (mostly spherical, less than 1 mm across) and lining some ITZ cracks with some ASR extrusion products as shown in Fig.4b. The evidence of gel extrusion from reactive aggregates, particular sericite, cut into the cracks around ITZ originally filled with DEF product as previously reported [16] also shown in Fig.3c. These showed that the results obtained from these techniques provided both useful information and possible clues as to the cause and timeline of the deterioration.

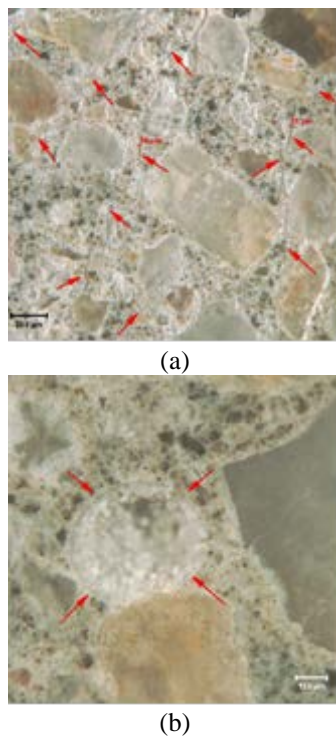


Fig.4 (a) microcracks in paste filled with ASR gel, (b) air void filled with ettringite

3.4 SEM/EDX

The morphological study of the products identified two types of gels as shown in Fig.5. Most amorphous gels, often with shrinkage cracks, were found in the cement paste cracks and in the ITZ as shown in back-scattered electron image in Fig.5a. Cryptocrystalline gels were normally found in internal cracks of sericite or also in some granitic

aggregates without cataclastic texture. Developed cryptocrystalline gel surrounded by gel in the reacted sericite aggregate is shown in Fig.5b.

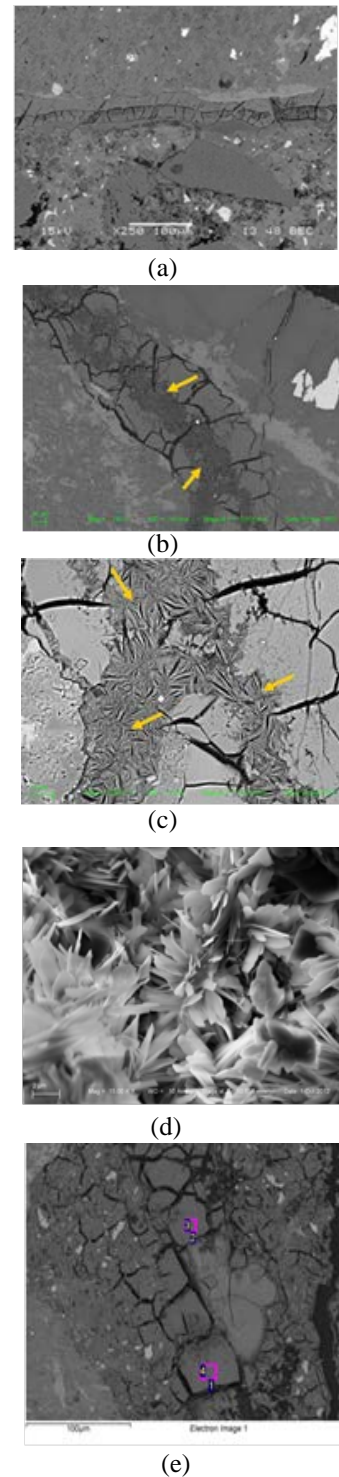


Fig.5 (a) internal microcrack in the paste, filled with ASR gel, (b) cryptocrystalline gel in the crack, (c) the detail of gel in (b), (d) the rosette form of a gel in sericite rock, (e) close-up of gel in cement paste

The enlarged area of Fig.5 is shown in Fig.5c and this shows cryptocrystalline globular reaction products (arrows) among the surrounding gel. These secondary crystalline products internally occurred in the crack and believed to be crystallized from the precursor gel. Fig.5d shows the existence of the plate-formed rosette crystals agglomerated from a fragment of sericite aggregate in this sample. The example of a detailed chemical analysis of the gel found in the crack in Fig.5e is shown in Table 2

Table 2 Detailed analysis of gel in each location of cement paste in Fig.5e

Processing option: Oxygen by Stoichiometry (Normalised)

Spectrum	In stats.	Mg	Al	Si	Ca	Total
1	No	1.21	1.81	92.1	4.89	100.0
2	No		2.10	92.4	5.50	100.0
3	No		3.39	92.1	4.47	100.0
4	No	1.25	3.12	01.1	4.49	100.0
Max.		0.00	0.00	0.00	0.00	
Min.		0.00	0.00	0.00	0.00	

Note: all results in compounds %

In general, gel products found in cracks in the cement paste were composed of silica, aluminum, and calcium, but the slightly different compositions were found in different observed areas. Gels found in cracks in reacted aggregates contained higher potassium and sodium compared to those in the paste and the ITZ. Alkali ions in gels found in cement paste were probably “reduced” by reacting with the cement paste as reported in the literature [17]

4. CONCLUSIONS

1. Several techniques can be combined and effectively used to identify ASR as the primary cause of deterioration and the continued expansion of the investigated structures.

2. Both simple qualitative screening tests agreed well with the results of other tests, particularly the expansion test, but other techniques must also be used for further confirmation.

3. The expansion test in different environments can identify the behaviors under the accelerated conditions which led to the suggested cause of the problem. The detailed studies from microstructure analysis, petrographic analysis and SEM/EDS confirmed the cause of the problem, identifying materials and significant features, in both qualitative and quantitative aspects.

4. Two forms of ASR gels were observed; amorphous gels found in the cracks in the cement paste, the ITZ and in some air voids, and

cryptocrystalline gels found mostly in the cracks inside the aggregates.

5. DEF was also found in cracks and air void, but there was no correlation to the continued expansion.

5. ACKNOWLEDGMENTS

The authors acknowledge funding supports from the Faculty of Engineering, Kasetsart University and Kasetsart University Research and Development Institute (KURDI) and technical support from Siam Research and Innovation Co., Ltd.,

6. REFERENCES

- [1] Stanton T.E., Influence of cement and aggregate on concrete expansion, Eng News-Rec. 123(5), 1940, pp. 59-61.
- [2] Stanton T.E., Expansion of concrete through a reaction between cement and aggregate, T Am Soc Civ Eng. 107(1), 1942, pp.54-84.
- [3] Thomas M., Dunster A., Nixon P. and Blackwell B., Effect of fly ash on the expansion of concrete due to alkali-silica reaction-exposure site studies, Cem. Concr Compos. 33, 2011, pp. 359-367.
- [4] RILEM Working Group (TC 191), Guide to diagnosis and appraisal of AAR damage to concrete in structures: Part 1 Diagnosis (AAR 6.1), in B. Godart, M.de Rooji, and J.G.M. Wood (Eds.), RILEM State-of-the Art-Reports vol. 12, 2013.
- [5] ASTM, Standard Test Method for Potential Alkali Reactivity of Aggregates (Mortar-Bar Method): ASTM C 1260, 2003.
- [6] Du-You L., Fournier B., and Grattan-Bellew P.E., Evaluation of the Chinese Accelerated Test for alkali-carbonate reaction, J. ASTM Int. 3, 2006, pp.1-10.
- [7] Sujjavanich S., Suwanvitaya P., and Rothstein D., Investigation of ASR in mass concrete structures: A case study, in S.O. Cheung, S. Yazdani, N. Ghafoori and A. Singh (Eds.), Modern Methods and Advances in Structural Engineering and Construction, 2011.
- [8] Sujjavanich, S., Won-In, K., Meesak, T., Wongkamjan, W., & Jensen, V. Investigation of Potential Alkali-Silica Reactivity of Aggregates Sources in Thailand, International Journal of GEOMATE, Vol.13, Issue 35, 2017. pp. 108-113.
- [9] Swamy R.N., The Alkali-Silica Reaction in Concrete. Taylor & Francis e-Library, 2003.
- [10] Grantham M.G., Gray M.J., and Eden M.A., Delayed ettringite formation in foundation bases, A case study, Structural Faults + Repair-99., 1999.

- [11] Famy C., Scrivener K.L., Atkinson A., and Brough A.R., Influence of the storage conditions on the dimensional changes of heat-cured mortars, *Cem.Conc. Res.* 31, 2001, pp. 795-803.
- [12] ASTM, Standard Practice for Petrographic Examination of Hardened Concrete, in Annual Book of ASTM Standards Vol 04.02 Concrete and Aggregates ASTM C 856 – 04, 2004.
- [13] Guthrie J.G.D., and Carey J.W., A simple environmentally friendly, and chemically specific method for the identification and evaluation of the alkali-silica reaction, *Cem.Conc. Res.* 21, 1997, pp.1407-1417.
- [14] ACI Committee 221, State-of-the-Art Report on Alkali-Aggregate Reactivity: ACI 221.1R-98, American Concrete Institute, 1998.
- [15] Jensen V., Alkali-aggregate reaction in Southern Norway, Doctoral, University of Trondheim (NTH), Trondheim, 1993.
- [16] Jensen V. and Sujjavanich S., ASR and DEF in the concrete foundation in Thailand, in Pro. of the 15th Int. Conf. on Alkali-Aggregate Reaction: Alkali-Aggregate Reactions in Concrete, Brazil, 2016.
- [17] Diamond S., R.S.Jr. Barney back, and L.J. Struble, Physics and chemistry of alkali-silica reactions, in Proc. of the 5th Int. Conf. on Alkali-Aggregate Reaction: Alkali-Aggregate Reactions in Concrete, South Africa, 1981.

Copyright © Int. J. of GEOMATE. All rights reserved, including the making of copies unless permission is obtained from the copyright proprietors.
